Review Article • DOI: 10.2478/s13380-013-0106-5 • Translational Neuroscience • 4(1) • 2013 • 59-65

VERSITA

DIFFUSION MR IMAGING: HOW TO GET THE MAXIMUM FROM THE EXPERIMENTAL TIME

Silvia De Santis[1,2*]

[1]*CUBRIC, School of Psychology, Cardiff University, UK*

[2]*Neuroscience & Mental Health Research Institute, Cardiff University, UK*

Abstract

Diffusion-based MR imaging is the only non-invasive method for characterising the microstructural organization of brain tissue *in vivo*. Diffusion tensor MRI (DT-MRI) is currently routinely used in both research and clinical practice. However, other diffusion approaches are gaining more and more popularity and an increasing number of researchers express interest in using them concomitantly with DT-MRI. While non tensor-based methods hold great promises for increasing the specificity of diffusion MR imaging, including them in the experimental routine inevitably leads to longer experimental times. In most cases, this may preclude the translation of the full protocol to clinical practice, especially when these methods are to be used with subjects that are not compatible with long scanning sessions (e.g., with elderly and pediatric subjects who have difficulties in maintaining a fixed head position during a long imaging session).

The aim of this review is to guide the end-users on obtaining the maximum from the experimental time allocated to collecting diffusion MRI data. This is done by: (i) briefly reviewing non tensor-based approaches; (ii) reviewing the optimal protocols for both tensor and non tensor-based imaging; and (iii) drawing the conclusions for different experimental times.

Keywords

• Diffusion tensor • MRI • Sampling schemes • Optimisation • Data quality • CHARMED • Tractography • Anomalous Diffusion

Received 14 November 2012
accepted 25 January 2013

Introduction

Diffusion MR Imaging (D-MRI) is a collection of non-invasive imaging techniques able to generate *in vivo* images of the brain, in which the contrast reflects the diffusion properties of the water molecules within the brain tissue.

The diffusion tensor MRI (DT-MRI) framework [1,2] uses the diffusion tensor to model diffusion data. To reconstruct the tensor, a collection of diffusion-weighted (DW) images are acquired using the same magnitude as the diffusion weighting, but applied along different spatial orientations. The DW magnitude is quantified by the so-called b-value, that takes into account the time in which the experiment is sensitive to the molecules' motion (Δ), and the field gradient strength (g) and duration (δ).

From the tensor, the mean diffusivity (MD), the average diffusivity in the voxel, and the fractional anisotropy (FA) which indicates the degree of anisotropy of the water molecules, are extracted. These are scalar parameters that reflect some of the features of the diffusion dynamics within a specific voxel. For example, white matter (WM) voxels with one prevalent fibre orientation exhibit high FA since diffusion is less hindered in the direction parallel to the fibres than perpendicular to them.

From the tensor, the direction of greatest diffusivity can also be extracted. This is interpreted as the main fibre orientation and fed into tractography reconstruction algorithms [3-8], that delineate the WM fiber pathways by merging this information in contiguous voxels. In this way, virtual dissection of WM can be performed non-invasively.

Numerous studies have been performed documenting the clinical utility of DT-MRI in various brain diseases (for a review, see [9]) and its ability to track specific patterns in the developing [10] as well as in the aging brain [11].

When it comes to interpreting the results, MD and FA are both dependent on several aspects of the local microstructure. 20 years after its first introduction, it is now clear that DT-MRI indices reflect the sum of different contributions that are impossible to disentangle using the diffusion tensor model. For a start, the tensor model is inadequate for characterising fibre orientation when there is more than one fibre population within a voxel, generating inaccurate tract reconstructions. The tensor is also modulated by the myelination and by the axonal properties (density and radius). This is why DT-MRI indices are considered very sensitive with respect to local changes in diffusivity properties, but not specific towards the cause of the observed change.

To overcome these issues, different approaches have been introduced over the years that use more complex models of the diffusion dynamics. From the point of view of the data collection, the signal needs to be acquired using more gradient orientations than DT-MRI, or more than one b-value, or both, so that including them in the experimental routine inevitably leads to longer experimental times.

Numerous approaches have been proposed in recent years or are currently under investigation, with the aim of rapidly image the entire brain with high degrees of precision in space and time. Although the benefit of these approaches have been documented, techniques such as multiplexing

* *E-mail: desantiss@cardiff.ac.uk*

[12], compressed sensing [13,14], and non EPI-based approaches such as PROPELLER [15], do not currently feature in clinical scan protocols, in which diffusion data is commonly acquired with the twice-refocused spin-echo EPI sequence [16]. Although this is likely to change in the next few years due to hardware developments, the scope of this review is to guide the end-users to obtain the maximum from the experimental time they can allocate to collect diffusion MRI data using the "off-the-shelf" methods that are most widely available in labs.

Specifically, non tensor-based approaches to diffusion will be reviewed in the next section. Then, optimal protocols for both tensor and non tensor-based methods will be revised, with the aim of defining minimal requirements to obtain an acceptable data quality in the shortest possible time. The last section will combine these requirements to guide the diffusion imager to get the most from the available experimental time.

Non tensor-based approaches to increase the information of D-MRI

Several diffusion methods are available today to resolve multiple fiber orientations, all of them relying on High Angular Resolution Diffusion Imaging, or HARDI, acquisition schemes (i.e., they use a large number of unique gradient orientations to acquire the data). The simplest generalisation of DT-MRI relies on fitting more than one tensor to the data, as done in [17,18]. More recently, frameworks to recover the fiber orientation distribution, i.e. the probability of finding fibres with a given orientation in the voxel, were introduced. There are two main strategies to recover the fiber orientation distribution: it can be extracted directly from the data using the mathematical properties of the diffusion signal, as done in Q-Ball imaging [19], Diffusion Spectrum Imaging (DSI) [20] or Persistent Angular Structure MRI [21], or by deconvolving the idealised response from a single fibre population, as done in spherical deconvolution-based approaches [22-24]. For a detailed review and comparison of these approaches, see [25].

To overcome the low specificity of DT-MRI indices, the signal can be expressed using higher order models with the purpose of extracting complementary parameters and relating the outcome to some biophysical models of the tissue. While the simplest generalization of DT-MRI to try to account for the possible existence of multiple components is a two-tensor model [26], it is not clear what, physically, the two tensor components would represent, given that biexponential fitting of diffusion-weighted signal-attenuation curves measured along a single orientation does not yield physical values for the intra and extra-cellular water fractions [27].

An approach that is growing in popularity is Diffusional Kurtosis Imaging (DKI) [28-30]. In this approach, the deviation from the exponential decay is quantified using a convenient dimensionless metric called the excess kurtosis, which is determined from the first three terms of an expansion of the logarithm of the NMR signal intensity in powers of the b-value. DKI has been largely applied in the last years, due to its clinical feasibility and to the enhanced sensitivity as compared to DT-MRI [28,31].

More recently, it has been proposed that this intrinsic non mono-exponential behaviour (where the tensor model implies an exponential decay of the signal as a function of the b-value) can be described by the anomalous diffusion (AD) framework [32] leading to a stretched-exponential model for the diffusion signal [33-37].

Hybrid approaches can be particularly useful for both recovering more than one fibre orientation within the voxel and for defining more tissue-specific properties. For example, the composite hindered and restricted model of diffusion, or CHARMED [38,39], explains the signal as the contribution of two different pools: a hindered extra-axonal compartment and one or more intra-axonal compartments, whose properties are characterised by a model of restricted diffusion perpendicular to fibre axis within impermeable cylinders [40]. This model provides distinct WM-specific parameters, e.g., the axonal density, and was recently extended to estimate the axonal diameter [41,42].

Optimal acquisition strategies for tensor and non tensor-based diffusion imaging

D-MRI involves DW data that are currently acquired using the twice-refocused spin-echo EPI sequence, a sequence designed to minimise the distortions caused by the rapid switching on and off of the gradients [16]. This is true for all the D-MRI techniques described so far, except for the CHARMED model that is implemented for the single-refocused version of the same sequence.

When using such pulse sequences, the experimenter normally has to select only two of the diffusion-related parameters, i.e., the b-value and the gradient orientations, because other parameters are selected automatically, as a consequence, to maximise the SNR by having the shortest echo time (TE) possible. Specifically, the gradient strength is always the largest that the scanner can provide, in order to minimise δ and, thus, the TE. In most cases, the optimal choice of Δ/δ is the value that, given the target b-value, minimises Δ in order to reduce the TE.

While the b-value has only a moderate effect on the total experimental time, the more gradient orientations, the more measurements required, the longer the experiment duration, and thus the optimal requirements in terms of number of gradient orientations will be the key feature for the purpose of this review. In addition, the terms 'gradient orientations' and 'measurements' will be interchangeable in this context.

The optimal b-value for DT-MRI in the brain falls in the range $750<b<1300$ s/mm^2, where different parameters (i.e., MD, FA and fiber orientations) need slightly different b-values within this range [43-45]. A b-value around 1000 s/mm^2 is considered to be an optimal choice to maximise precision in the key parameters extracted from DT-MRI.

The diffusion tensor has six unknown parameters, hence six is the minimum number of unique gradient orientations needed for tensor reconstruction (plus at least one non-DW scan). When time permits, more orientations should be acquired, resulting in a overdetermined system that permits a

more robust tensor estimation. More unique orientations are preferred compared to multiple repeats of the same orientation to maximize the statistical rotational invariance on DTI estimates, i.e. the dependence of the uncertainty in parameters as a function of orientation of the structure with respect to the encoding gradients [46,47].

According to published works, 20 or more unique orientations are ideal to maximise the precision for FA [48], while 30 or more unique orientations are needed for obtaining robust estimates of the trace and the principal eigenvector orientation. In addition, the gradient sampling vectors should be distributed in space as uniformly as possible so as to aim for an average SNR that is as uniform as possible, irrespective of the fibre orientation [47]. The gradient sampling scheme is conventionally visualised as spots lying on a sphere, where the radius is proportional to the amount of diffusion weighting and the different orientations are illustrated as points placed where the line intersects the surface of the sphere. Lastly, the ratio of measurements made with DW to those without should be around 8-10:1 [43]. For a comprehensive review on optimal acquisition methods for DT-MRI, please refer to [49].

Whilst there is an extensive literature on optimal schemes for DT-MRI, it is very difficult to indicate general guidelines for performing non DT-MRI experiments, since the design is specific to the different techniques mentioned above and very few works have been published on this topic.

A visual summary of the differential requirements of the techniques described so far is shown in Figure 1. Figure 1 is a 2D pictorial representation of the 3D sphere conventionally used to visualise the gradient sampling scheme. More orientations increase the angular resolution; more concentric spheres or shells increase the sampling of the b-value or gradient space. Some techniques use a single shell approach like DT-MRI (Figure 1a), i.e., all the gradient orientations have the same b-values and can thus be graphically represented as lying on the surface of a sphere. Others (and definitely all the techniques fitting more than one compartment) need more than one b-value and thus they are considered multi-shells techniques. Methods that are focused on resolving multiple fiber orientations needs high angular resolution (Figure 1b), while methods that fit the diffusion signal using multiple compartments or expressions more complex than the exponential decay need increased sampling of the b-value space (Figure 1c and 1d). The requirements for DSI are different in that it needs a cartesian grid sampling scheme, since it involves a Fourier transform of the data in the gradient space. Hence, both high angular resolution and high b-value sampling rate are needed (Figure 1e).

DKI analysis implies fitting two tensors to the data: the diffusion tensor and the kurtosis tensor. While the first one has 6 degrees of freedom, the second has 15 degrees of freedom, thus at least 22 unique acquisitions are needed (including the volume with no DW). It can be further shown that there must be, in general, at least two distinct b-values, and that the maximum b-value should be smaller than 3000 [30].

Optimal acquisition schemes for DSI were investigated in ref. [50]. The optimal maximum b-value is 6500 s/mm^2 for DSI with 515 measurements and 4000 s/mm^2 for DSI with 203 measurements. Both schemes provide a maximum distinguishable crossing angle of 30 degrees. More recently, as a result of the introduction of compressed sensing [13], DSI was successfully performed using only 100 diffusion measurements for the b=4000 scheme [51]. For DSI, the suggestion of having the shortest possible Δ (that leads to Δ~δ) should not be followed because being in the so-called narrow pulse regime (i.e., Δ>>δ) is a prerequisite for performing the Fourier transform. Ref [50] suggests Δ=80 and δ=35.

Methods based on spherical deconvolution usually need single shell acquisitions. A b-value higher than the one employed for DT-MRI should be used, given that the angular dependency of signal is more pronounced at higher b-values [52-54], so generally b=3000 s/mm^2 is used. In methods based on spherical deconvolution, the minimum number of measurements is given by the maximum order of harmonics that are used in the data analysis. Simulations show that the signal profile at b=3000 s/mm^2 only need 28 unique measurements, while *in vivo* data contains higher angular frequency components, therefore suggesting a minimum of 45 unique measurements [55]. However, as pointed out in [49], these numbers are only minimal requirements. When time allows, more measurements should be collected, resulting in a overdetermined system that permits a more robust fit. To the best of the Author's knowledge, the maximum distinguishable angle for crossing fibres as a function of the number of unique measurements is still an open question.

For hybrid models based on hindered and restricted diffusion, Alexander et al. proposed a framework to optimise the sequence parameters by keeping the diffusion gradient

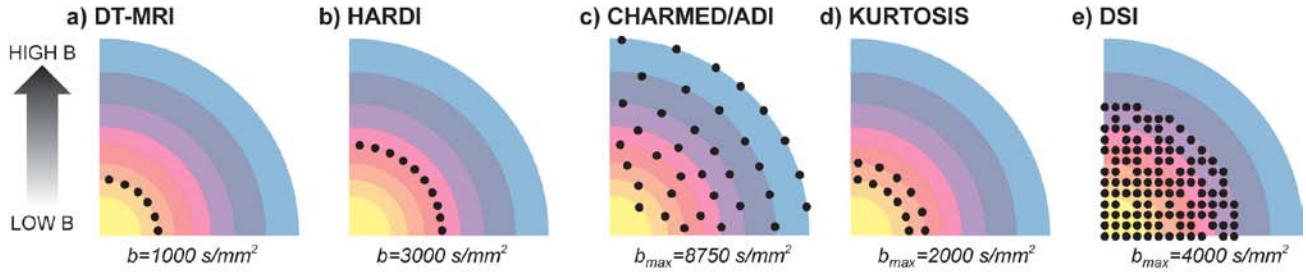

Figure 1. Five different acquisition schemes illustrated in the text: DT-MRI (a), single shell HARDI (b), CHARMED/ADI (c), Kurtosis (d) and DSI (e). All the schemes have a shell structure except the DSI scheme, which employs instead a (undersampled) cartesian grid.

orientations fixed and distributed evenly on the unit hemisphere [56,57]. Following works showed that having more gradient orientations in the high b-value shells improves the precision and accuracy on the estimated parameters [58]. The optimised protocol proposed in [58] employs 45 unique measurements.

In methods based on the anomalous diffusion framework, a stretched exponential decay is fitted to the data, and thus multi-shell acquisition is required. Since no specific optimisation has been made so far for anomalous diffusion acquisitions, we assume that the multi-shell optimisation performed for CHARMED-like acquisition is also valid for anomalous diffusion imaging, i.e., from a single protocol employing 45 unique measures, one can obtain both CHARMED-like parameters and anomalous diffusion parameters. This last issue requires further validation.

Get the maximum from the experimental time

The acquisition time for a single measurement is mainly dictated by the repetition time (TR). The minimum TR value is affected by several factors, and should always be at least 5 times the T1, which will allow the magnetization to relax to 99% of its initial value and avoid T1-weighting effects. In the human brain at 3T, TR~1.2s and thus 5*TR~6s [59]. TR depends on the number of phase encoding steps, and thus on the geometry and on the acquisition strategy (i.e., the use of parallel imaging allows shorter TR by reducing the number of phase encoding steps). Higher spatial resolution and larger volumes need a longer TR.

Throughout this section, we will assume TR=17s, which is the TR that allows a whole brain acquisition at 2.4 mm isotropic resolution on a GE Signa 3T (ASSET factor=2). Acquisition times for different setups are expected to vary, but they can easily be worked out accounting for the actual TR. All the calculations in this paragraph do not include cardiac gating [60], that should be employed when time allows, and the non-DW scans, that should be added at the beginning of the acquisition.

In principle, since most of the diffusion acquisitions are performed using the same pulse sequence, the experimenter may want to perform a single experiment by adding up the gradient orientations/b-values required by each technique he/she is interested in as continuous sequence, specifying a single TE/TR and a single geometry. This is not recommended because combining techniques that need different b-values lead to an increased TE (the common TE will be dictated by the highest b-value), and thus a decrease of the SNR for all the acquisitions. Combining acquisitions with different TEs is possible if all the DW images are divided by the corresponding non-DW scan, but not desirable in many cases (e.g., if running multi-compartment model fit, the acquisition has to have the same TE to weight equally each compartment).

A visual summary of the three proposed protocols is reported in Figure 2.

D-MRI in 45 minutes or more

When long scanning is not an issue and the experimenter is interested in having the most compete picture obtainable using D-MRI, then different protocols should be included. To obtain robust maps of MD and FA, the experimenter should use a DT-MRI protocol with 30 unique gradient orientations and a b-value around 1000 s/mm^2. If the SNR is high enough, so that the TE can be increased to include another set of 30 measurements with a b-value around 2000 s/mm^2, then a combined DT-MRI and DKI can be performed, with 60 measurements in total. For tractography reconstruction, a HARDI protocol with at least 45 unique gradient orientations and a b-value of 3000 s/mm^2 should be included. Alternatively, DSI protocol can be applied, implying 100 measurements with b=4000 s/mm^2. Higher order model of diffusion (i.e., AD and CHARMED) can be estimated using the scheme proposed in [58] with 45 unique measurements and a maximum b-value of 8750 s/mm^2. Assuming TR=17s, this will result in a total acquisition time of 42 minutes using HARDI or 58 minutes using DSI.

D-MRI in 30 minutes

If the time available for diffusion scanning is around 30 minutes, the HARDI single-shell protocol should be preferred over multi-shell

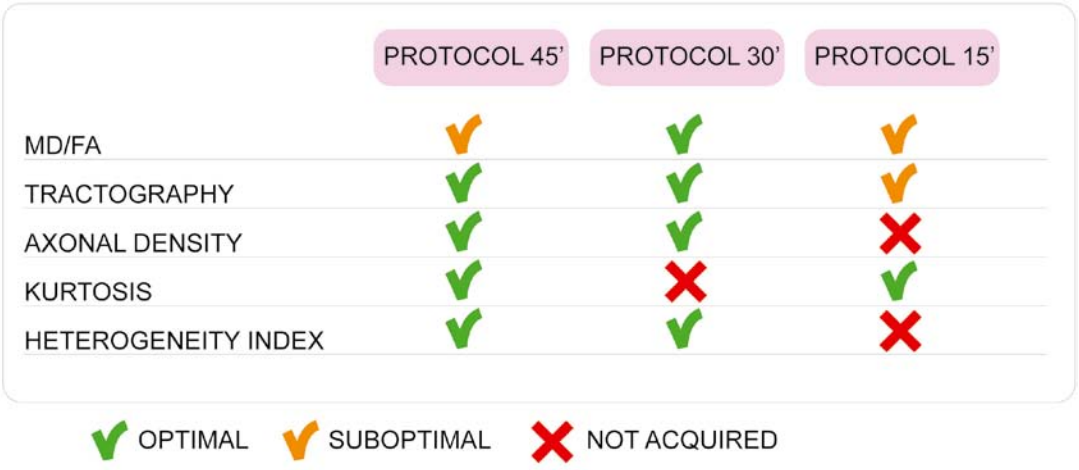

Figure 2. Three different acquisition protocols illustrated in the text. Green check means that the acquisition is performed according to the optimal protocol while orange indicates the use of a sub-optimal scheme to reduce the acquisition time. Red cross means that it is not possible to acquire the protocol in the allocated experimental time.

approaches like DSI. One can still allocate time for the AD/CHARMED protocol and infer about the kurtosis values, remembering that in coherent white matter fibers there is a high correlation between the axonal density from CHARMED and the kurtosis [61]. Assuming TR=17s, this will result in a total acquisition time of 34 minutes.

D-MRI in 15 minutes

If the time available for diffusion scanning is limited to 15 minutes, one can still measure both tensor and non-tensormetrics in the brain. An effective way is to use an acquisition protocol with 30 orientations at two b-values, one around 1000 and the other around 2000 s/mm^2, i.e., a combined DT-MRI and DKI protocol. Accepting the trade-off on the SNR, both DT-MRI and kurtosis indices can be measured. In addition, the shell with the largest b-value can be used for tractography reconstruction, where 28 unique measurements are sufficient to account for the angular frequency component up to b=3000 s/mm^2 in methods based on spherical deconvolution. Assuming TR=17s, this will result in a total acquisition time of 16 minutes.

Conclusions and perspectives

In this review article, optimal approaches to obtain quantitative diffusion imaging of the brain are revised, with the purpose of guiding the end-users to obtain the maximum from the experimental time they can allocate to collect diffusion MRI data. As a result, three protocols are suggested with different demands in terms of experimental time (45, 30 and 15 minutes), offering a combination of conventional and non-conventional diffusion imaging.

A more widespread use of non-tensor based techniques is expected to have a large impact on the ability to elucidate brain morphology in health, development and disease. Surgical planning is improved when using HARDI-based tractography, by increased accuracy in tract reconstruction [62]. Kurtosis indices are more sensitive to myelin changes than DT-MRI parameters [63,64], and can play a role in the diagnosis of demyelinating pathologies like multiple sclerosis. CHARMED indices have been shown to be more sensitive than DT-MRI to micro-structural changes in short term neuro-plasticity [65]. Lastly, AD indices are also sensitive to local susceptibility differences between tissues [66]. This suggests possible applications in neurodegenerative pathologies involving iron accumulation, including Alzheimer's disease [67].

To summarise, diffusion MRI techniques hold great promise for increasing the information content of brain imaging analyses. This review article can help orient the scientific community towards a wider applicability and translation of these methods.

Acknowledgements

The author wishes to thank Prof. D. K. Jones and all the diffusion group of CUBRIC, Cardiff University for useful discussions and suggestions.

Funding

This work was supported by the Wellcome Trust through a Sir Henry Wellcome Postdoctoral Fellowship.

References

[1] Basser P. J., Mattiello J., LeBihan D., Estimation of the effective self-diffusion tensor from the NMR spin echo, J. Magn. Reson. B, 1994, 103, 247–254

[2] Basser P. J., Inferring microstructural features and the physiological state of tissues from diffusion-weighted images, NMR Biomed., 1995, 8, 333–344

[3] Conturo T. E., Lori N. F., Cull T. S., Akbudak E., Snyder A. Z., Shimony J. S., et al., Tracking neuronal fiber pathways in the living human brain, Proc. Natl. Acad. Sci. USA, 1999, 96, 10422–10427

[4] Jones D. K., Simmons A., Williams S. C., Horsfield M. A., Non-invasive assessment of axonal fiber connectivity in the human brain via diffusion tensor MRI, Magn. Reson. Med., 1999, 42, 37–41

[5] Mori S., Crain B. J., Chacko V. P., van Zijl P. C., Three-dimensional tracking of axonal projections in the brain by magnetic resonance imaging, Ann. Neurol., 1999, 45, 265–269

[6] Basser P. J., Pajevic S., Pierpaoli C., Duda J., Aldroubi A., In vivo fiber tractography using DT-MRI data, Magn. Reson. Med., 2000, 44, 625–632

[7] Parker G. J., Haroon H. A., Wheeler-Kingshott C. A., A framework for a streamline-based probabilistic index of connectivity (PICo) using a structural interpretation of MRI diffusion measurements, J. Magn. Reson. Imaging, 2003, 18, 242–254

[8] Poupon C., Mangin J., Clark C. A., Frouin V., Régis J., Le Bihan D., et al., Towards inference of human brain connectivity from MR diffusion tensor data, Med. Image Anal., 2001, 5, 1–15

[9] Assaf Y., Pasternak O., Diffusion tensor imaging (DTI)-based white matter mapping in brain research: a review, J. Mol. Neurosci., 2008, 34, 51–61

[10] Hüppi P. S., Dubois J., Diffusion tensor imaging of brain development, Semin. Fetal Neonatal Med., 2006, 11, 489–497

[11] Pfefferbaum A., Sullivan E. V., Hedehus M., Lim K. O., Adalsteinsson E., Moseley M., Age-related decline in brain white matter anisotropy measured with spatially corrected echo-planar diffusion tensor imaging, Magn. Reson. Med., 2000, 44, 259–268

[12] Feinberg D. A., Moeller S., Smith S. M., Auerbach E., Ramanna S., Gunther M., et al., Multiplexed echo planar imaging for sub-second whole brain fmri and fast diffusion imaging, PLoS One, 2010, 5, e15710

[13] Lustig M., Donoho D., Pauly J. M., Sparse MRI: the application of compressed sensing for rapid MR imaging, Magn. Reson. Med., 2007, 58, 1182–1195

[14] Menzel M. I., Tan E. T., Khare K., Sperl J. I., King K. F., Tao X., et al., Accelerated diffusion spectrum imaging in the human brain using compressed sensing, Magn. Reson. Med., 2011, 66, 1226–1233

[15] Pipe J. G., Farthing V. G., Forbes K. P., Multishot diffusion-weighted FSE using PROPELLER MRI, Magn. Reson. Med., 2002, 47, 42–52
[16] Reese T. G., Heid O., Weisskoff R. M., Wedeen V. J., Reduction of eddy-current-induced distortion in diffusion MRI using a twice-refocused spin echo, Magn. Reson. Med., 2003, 49, 177–182
[17] Tuch D. S., Reese T. G., Wiegell M. R., Makris N., Belliveau J. W., Wedeen V. J., High angular resolution diffusion imaging reveals intravoxel white matter fiber heterogeneity, Magn. Reson. Med., 2002, 48, 577–582
[18] Behrens T. E., Berg H. J., Jbabdi S, Rushworth M. F., Woolrich M. W., Probabilistic diffusion tractography with multiple fibre orientations: what can we gain?, Neuroimage, 2007, 34, 144–155
[19] Tuch D., S., Q-ball imaging, Magn. Reson. Med., 2004, 52, 1358–1372
[20] Wedeen V. J., Hagmann P., Tseng W.Y., Reese T. G., Weisskoff R. M., Mapping complex tissue architecture with diffusion spectrum magnetic resonance imaging, Magn. Reson. Med., 2005, 54, 1377–1386
[21] Jansons K. M., Alexander D. C., Persistent angular structure: new insights from diffusion MRI data. Dummy version, Inf. Process. Med. Imaging, 2003, 18, 672–683
[22] Tournier J. D., Calamante F., Gadian D. G., Connelly A., Direct estimation of the fiber orientation density function from diffusion-weighted MRI data using spherical deconvolution, Neuroimage, 2004, 23, 1176–1185
[23] Tournier J. D., Calamante F., Connelly A., Robust determination of the fibre orientation distribution in diffusion MRI: non-negativity constrained super-resolved spherical deconvolution, Neuroimage, 2007, 35, 1459–1472
[24] Dell'acqua F., Scifo P., Rizzo G., Catani M., Simmons A., Scotti G., et al., A modified damped Richardson-Lucy algorithm to reduce isotropic background effects in spherical deconvolution, Neuroimage, 2010, 49, 1446–1458
[25] Alexander D. C., Seunarine K. K, Mathematics of crossing fibers (chapter 27), In: Jones D. K. (Ed.), Diffusion MRI: theory, methods, and applications, Oxford University Press, New York, 2011
[26] Maier S. E., Vajapeyam S., Mamata H., Westin C. F., Jolesz F. A., Mulkern R. V., Biexponential diffusion tensor analysis of human brain diffusion data, Magn. Reson. Med., 2004, 51, 321–330
[27] Nicholson C., Syková E., Extracellular space structure revealed by diffusion analysis, Trends Neurosci., 1998, 21, 207–215
[28] Jensen J. H., Helpern J. A., Ramani A., Lu H., Kaczynski K., Diffusional kurtosis imaging: the quantification of non-Gaussian water diffusion by means of magnetic resonance imaging, Magn. Reson. Med., 2005, 53, 1432–1440
[29] Lu H., Jensen J. H., Ramani A., Helpern J. A., Three-dimensional characterization of non-Gaussian water diffusion in humans using diffusion kurtosis imaging, NMR Biomed., 2006, 19, 236–247
[30] Jensen J. H., Helpern J.A., MRI quantification of non-Gaussian water diffusion by kurtosis analysis, NMR Biomed., 2010, 23, 698–710
[31] Wu E. X., Cheung M. M., MR diffusion kurtosis imaging for neural tissue characterization, NMR Biomed., 2010, 23, 836–848
[32] Metzler R., Klafter J., The random walk's guide to anomalous diffusion: a fractional dynamics approach, Phys. Rep., 2000, 339, 1–77
[33] Bennett K. M., Schmainda K. M., Bennett R. T., Rowe D. B., Lu H., Hyde J.S., Characterization of continuously distributed cortical water diffusion rates with a stretched-exponential model, Magn. Reson. Med., 2003, 50, 727–734
[34] Ozarslan E., Basser P. J., Shepherd T. M., Thelwall P. E., Vemuri B. C., Blackband S. J., Observation of anomalous diffusion in excised tissue by characterizing the diffusion-time dependence of the MR signal, J. Magn. Reson., 2006, 183, 315–323
[35] Hall M. G., Barrick T. R., From diffusion-weighted MRI to anomalous diffusion imaging, Magn. Reson. Med., 2008, 59, 447–455
[36] Magin R. L., Abdullah O., Baleanu D., Zhou X. J., Anomalous diffusion expressed through fractional order differential operators in the Bloch-Torrey equation, J. Magn. Reson., 2008, 190, 255–270
[37] De Santis S., Gabrielli A., Bozzali M., Macaluso E., Maraviglia B., Capuani S., Anisotropic anomalous diffusion assessed in the human brain by scalar invariant indices, Magn. Res. Med., 2011, 65, 1043–1052
[38] Assaf Y., Freidlin R. Z., Rohde G. K., Basser P. J., New modeling and experimental framework to characterize hindered and restricted water diffusion in brain white matter, Magn. Reson. Med., 2004, 52, 965–978
[39] Assaf Y., Basser P. J., Composite hindered and restricted model of diffusion (CHARMED) MR imaging of the human brain, Neuroimage, 2005, 27, 48–58
[40] Neuman C. H., Spin echo of spins diffusing in a bounded medium, J. Chem. Phys., 1974, 60, 4508–4511
[41] Barazany D., Basser P. J., Assaf Y., In vivo measurement of axon diameter distribution in the corpus callosum of rat brain, Brain, 2009, 132, 1210–1220
[42] Alexander D. C., Hubbard P. L., Hall M. G., Moore E. A., Ptito M., Parker G. J., et al., Orientationally invariant indices of axon diameter and density from diffusion MRI, Neuroimage, 2010, 52, 1374–1389
[43] Jones D. K., Horsfield M. A., Simmons A., Optimal strategies for measuring diffusion in anisotropic systems by magnetic resonance imaging, Magn. Reson. Med., 1999, 42, 515–525
[44] Armitage P. A., Bastin M. E., Utilizing the diffusion-to-noise ratio to optimize magnetic resonance diffusion tensor acquisition strategies for improving measurements of diffusion anisotropy, Magn. Reson. Med., 2001, 45, 1056–1065
[45] Alexander D. C., Barker G. J., Optimal imaging parameters for fiber-orientation estimation in diffusion MRI, Neuroimage, 2005, 27, 357–367
[46] Conturo T. E., McKinstry R. C., Akbudak E., Robinson B. H., Encoding of anisotropic diffusion with tetrahedral gradients: a general mathematical diffusion formalism and experimental results, Magn. Reson. Med., 1996, 35, 399–412
[47] Jones D. K., The effect of gradient sampling schemes on measures derived from diffusion tensor MRI: a Monte Carlo study, Magn. Reson. Med., 2004, 51, 807–815

[48] Papadakis N. G., Murrills C. D., Hall L. D., Huang C. L., Carpenter T. A., Minimal gradient encoding for robust estimation of diffusion anisotropy, Magn. Reson. Imaging, 2000, 18, 671–679

[49] Jones D. K. (Ed.), Diffusion MRI: theory, methods and applications, Oxford University Press, New York, 2011

[50] Kuo L. W., Chen J. H., Wedeen V. J., Tseng W. Y., Optimization of diffusion spectrum imaging and q-ball imaging on clinical MRI system, Neuroimage, 2008, 41, 7–18

[51] Lee N., Wilkins B., Singh M., Accelerated diffusion spectrum imaging via compressed sensing for the human connectome project, Proc. SPIE 8314, Medical Imaging 2012: Image Processing, 83144G, doi: 10.1117/12.911569

[52] Alexander A. L., Hasan K. M., Lazar M., Tsuruda J. S., Parker D. L., Analysis of partial volume effects in diffusion-tensor MRI, Magn. Reson. Med., 2001, 45, 770–780

[53] Akazawa K., Yamada K., Matsushima S., Goto M., Yuen S., Nishimura T., Optimum b value for resolving crossing fibers: a study with standard clinical b value using 1.5-T MR, Neuroradiology, 2010, 52, 723-728

[54] Pannek K., Mathias J. L., Bigler E. D., Brown G., Taylor J. D., Rose S., An automated strategy for the delineation and parcellation of commissural pathways suitable for clinical populations utilising high angular resolution diffusion imaging tractography, Neuroimage, 2010, 50, 1044–1053

[55] Tournier J. D., Calamante F., Connelly A., How many diffusion gradient directions are required for HARDI?, Proc. Intl. Soc. Mag. Reson. Med., Hawai'i, 2009, 17p

[56] Alexander D. C., A general framework for experiment design in diffusion MRI and its application in measuring direct tissue-microstructure features, Magn. Reson. Med., 2008, 60, 439–448

[57] Zhang H., Schneider T., Wheeler-Kingshott C. A., Alexander D. C., NODDI: practical in vivo neurite orientation dispersion and density imaging of the human brain, Neuroimage, 2012, 61, 1000–1016

[58] De Santis S., Assaf Y., Evans C. J., Jones D. K., Improved precision in charmed assessment of white matter through sampling scheme optimisation and model parsimony testing, Magn. Res. Med., 2013 (in press)

[59] Deoni S. C., Rutt B. K., Arun T., Pierpaoli C., Jones D. K., Gleaning multicomponent T1 and T2 information from steady-state imaging data, Magn. Reson. Med., 2008, 60, 1372–1387

[60] Pierpaoli C., Marenco S., Rohde G., Jones D. K., Barnett A. S., Analysing the contribution of cardiac pulsation to the variability of quantities derived from the diffusion tensor, Proceedings of the 11th Annual Scientific Meeting of the International Society for Magnetic Resonance in Medicine, Toronto, Canada, 2003, abstract 70

[61] De Santis S., Assaf Y., Jones D. K., Using the biophysical CHARMED model to elucidate the underpinnings of contrast in diffusional kurtosis analysis of diffusion-weighted MRI, MAGMA, 2012, 25, 267–276

[62] Berman J., Diffusion MR tractography as a tool for surgical planning, Magn. Reson. Imaging Clin. N. Am., 2009, 17, 205–214

[63] Bar-Shir A., Duncan I. D., Cohen Y., QSI and DTI of excised brains of the myelin-deficient rat, Neuroimage, 2009, 48, 109–116

[64] Cheung M. M., Hui E. S., Chan K. C., Helpern J. A., Qi L., Wu E. X., Does diffusion kurtosis imaging lead to better neural tissue characterization? A rodent brain maturation study, Neuroimage, 2009, 45, 386-392

[65] Tavor I., Hofstetter S., Ben-Amitay S., Assaf Y., Investigation tissue micro-structure changes in short term neuro-plasticity with diffusion mri. Proceedings of the 19th Annual Scientific Meeting of the International Society for Magnetic Resonance in Medicine, Montreal, Quebec, Canada, 2011, abstract 415

[66] Palombo M., Gabrielli A., De Santis S., Cametti C., Ruocco G., Capuani S., Spatio-temporal anomalous diffusion in heterogeneous media by nuclear magnetic resonance, J. Chem. Phys., 2011, 135, 034504

[67] Pankhurst Q., Hautot D., Khan N., Dobson J., Increased levels of magnetic iron compounds in Alzheimer's disease, J. Alzheimers Dis., 2008, 13, 49-52